Dyes and Pigments 84 (2009) 95–101

Contents lists available at ScienceDirect

Dyes and Pigments

journal homepage: www.elsevier.com/locate/dyepig

An efficient light-harvesting ruthenium dye for solar cell application

Shi-Jhang Wu [a], Chia-Yuan Chen [a], Jian-Ging Chen [b], Jheng-Ying Li [a], Yung-Liang Tung [c], Kuo-Chuan Ho [b,*], Chun-Guey Wu [a,*]

[a] Department of Chemistry, National Central University, Jhong-Li 32001, Taiwan, ROC
[b] Department of Chemical Engineering, National Taiwan University, Taipei, 10617 Taiwan, ROC
[c] Photovoltaics Technology Center, Industrial Technology Research Institute (ITRI), Hsin-Chu, 310 Taiwan, ROC

ARTICLE INFO

Article history:
Received 20 March 2009
Received in revised form
29 June 2009
Accepted 30 June 2009
Available online 5 July 2009

Keywords:
Ruthenium
Heteroleptic
Dye-sensitized solar cell
Thiophene
Conjugation
High-efficiency

ABSTRACT

A novel, heteroleptic ruthenium dye comprising a vinyl group between the carboxylate and bipyridine segments as well as extended π-conjugation of the ancillary ligand, employing alkyl-bithiophene, was synthesized. The dye displayed a remarkably high absorption coefficient of 2.51×10^4 M^{-1} cm^{-1} (at 562 nm) for its metal-to-ligand charge transfer band. The photo-to-current conversion efficiency of the corresponding dye-sensitized solar cell was 9.12% under AM 1.5 (100 mW/cm^2) irradiation. Furthermore, owing to both the very strong metal-to-ligand charge transfer band and the large number of dye molecules adsorbed on the TiO_2 electrode, the conversion efficiency of the dye-sensitized cell was >7.5% at a light intensity ≤198 mW cm^{-2}.

1. Introduction

Dye-sensitized solar cells (DSC) are a promising candidate for photovoltaic technology by virtue of their high photon-to-current conversion efficiency and low manufacturing cost [1]. DSC with efficiencies >10% was first demonstrated in 1993 by Grätzel et al. [2] using cis-di(thiocyanato)bis-(2,2′-bipyridyl-4,4′- dicarboxylate) ruthenium(II) (**N3**) as a sensitizer. However, a major drawback of **N3** is its relatively low light-absorption ability within the visible and near-infrared regions [3,4]. Thus, the search for high-efficiency dye molecules, which has included ruthenium complexes [5–8], metal-free dyes [9–16] and metallo-porphyrins [17,18], has focused on increasing the dye's light-harvesting capacity and red-shifting its absorption profile. It was shown [19–24] that one of the best ways to enhance both the absorption coefficient and red-shift of the metal-to-ligand charge transfer (MLCT) band in a ruthenium-based photosensitizer, was to extend the π-conjugation length of the colorant's ancillary [19–22] or anchoring [23,24] ligands.

Previously, the current authors have prepared several heteroleptic ruthenium complexes by extending the conjugation length of the ancillary ligand [25,26]. Such heteroleptic ruthenium complexes have a strong MLCT band and DSC devices based on them display very good photovoltaic performance. Nevertheless, further extention of the conjugation length of the ancillary ligand faces the situation that the π-orbital energy of the ancillary ligand increases to match that of the metal center, with the result that the π orbital of the ancillary ligand participates, significantly, in the HOMO of the complex. This reduces the absorption coefficient of the MLCT band and therefore decreases efficiency, as shown previously [21]. To overcome this problem, a novel, heteroleptic ruthenium photosensitizer: (cis-di(thiocyanato)(4,4′-di-octyl-bithienyl)-2,2′-bipyri- dine) (4,4′-di-carboxylvinyl- 2,2′-bipyridine) ruthenium(II) (**CYC-B5**) was designed and synthesised. Compared to **N3**, **CYC-B5**, both ancillary and anchoring ligands possesses extended conjugation length; however, when compared to **CYC-B1** [25] which was reported previously, only the conjugation length of the anchoring ligand was extended. The UV/Vis spectra of **CYC-B5**, **N3** and **CYC-B1** revealed that the light-absorption capacity of a ruthenium photosensitizer can be increased by extending the conjugation length of both the anchoring and ancillary ligands simultaneously.

2. Experimental

2.1. Chemicals

Anhydrous lithium iodide, iodine, poly(ethylene glycol) (PEG), and *tert*-butylpyridine were obtained from Merck Co. Titanium (IV)

* Corresponding author. Tel.: +886 3 4227151x65903; fax: +886 3 4227664.
E-mail address: t610002@cc.ncu.edu.tw (C.-G. Wu).

0143-7208/$ – see front matter © 2009 Elsevier Ltd. All rights reserved.
doi:10.1016/j.dyepig.2009.06.017

isopropoxide (TTIP) (>98%) and 2-methoxylethanol (ME) were purchased from Acros Co. Acetonitrile was purchased from Merck Co. and dried with molecular sieves (4 Å). (*cis*-Di(thiocyanato)bis-(2,2′-bipyridyl-4,4′-dicarboxylate) ruthenium(II)) (**N3**) was a commercial product obtained from Solaronix SA, Aubonne, Switzerland. All other chemicals used were purchased from the commercial resources and were used without further treatment.

2.2. Preparation of *CYC-B5*

4,4′-dicarboxyvinyl-2,2′-bipyridine (**dcvbpy**) and alkyl-bithiophenes substituted bipyridine (**abtpy**) were prepared according to the literatures [24,25]. **CYC-B5**, (Ru[(dcvbpy)(abtpy)(NCS)$_2$]), was synthesized with a typical one-pot synthetic procedure reported previously [25]. 0.43 g (0.706 mmol) of [RuCl$_2$(p-cymene)]$_2$, 1.00 g (1.412 mmol) of **abtpy**, 0.42 g (1.412 mmol) of **dcvbpy** and excess NH_4NCS were mixed in a reaction vessel and the product was purified with Sephadex LH-20 using methanol as an eluent. After purification, 0.69 g (0.564 mmol) of **CYC-B5** was obtained with the yield of 39.9%. ^{1}H NMR (500 MHz, δ_H/ppm in d_6-DMSO, *J* Hz): 9.26 (d, 1H, 5.8); 9.15 (2 protons); 9.05 (s, 1H); 8.99 (s, 1H); 8.91 (s, 1H); 8.22 (2 protons); 8.15 (d, 1H, 5.7); 8.02 (d, 1H, 3.8); 7.80 (d, 1H, 15.9); 7.73 (d, 1H, 6.0); 7.55 (d, 1H, 15.9); 7.51 (d, 1H, 3.8); 7.48 (2 protons); 7.39 (2 protons); 7.34 (d, 1H, 3.4); 7.25 (d, 1H, 3.4); 7.21 (d, 1H, 16.0); 6.98 (d, 1H, 16.0); 6.90 (d, 1H, 3.3); 6.84 (d, 1H, 3.3); 2.81 (t, 2H, 8.4); 2.78 (t, 2H, 7.4); 1.65 (t, 2H, 7.4); 1.62 (t, 2H, 8.4); 1.26 (m, 20H); 0.85 (m, 6H). ^{13}C NMR (500 MHz, δ/ppm in d_6-DMSO): 166.92; 166.79; 158.70; 158.31; 157.49; 156.91; 152.41; 152.36; 152.12; 151.53; 146.29; 146.20; 141.58; 140.85; 140.63; 149.37; 140.27; 139.87; 139.83; 139.52; 136.79; 136.30; 134.28; 133.77; 133.13 (C of NCS); 132.95 (C of NCS′); 129.96; 129.91; 129.75; 129.66; 125.91; 125.84; 125.46; 124.89; 124.99; 124.90; 124.75; 124.70; 121.10; 121.35; 121.23; 120.83; 118.39; 118.17; Aliphatic carbon: 31.19; 30.91; 29.31; 29.25; 28.61; 28.57; 28.32; 22.96; 22.01; 21.99; 13.86; 13.41. MS: *m*/*z* 1222.2 ([M]$^+$) LRFAB-MS found: *m*/*z* 1222.2 (m) ([M]$^+$); 1164.2 (s) ([M-NCS]$^+$); HRFAB-MS found: 1222.2004. Elemental anal. calcd. for $C_{60}H_{60}N_6O_4S_6Ru$: C, 58.94%; H, 4.95%; N, 6.87%. Found: C, 58.82%; H, 5.79%; N, 6.43%.

2.3. Physicochemical measurements

^{1}H NMR spectra were recorded with a Bruker DRX-500 NMR spectrometer in d_6-DMSO. FAB-MS spectra were obtained using JMS-700 HRMS. UV/Vis spectra were measured using a Cary 300 Bio spectrometer. Electrochemical study of the metal complexes in solution was performed in a single-compartment, three-electrode cell with a platinum disk working electrode and a Pt wire counter electrode. The reference electrode was Ag/$AgNO_3$ and the supporting electrolyte was 0.1 M tetrabutyl-ammonium tetrafluoroborate ($TBABF_4$) in DMF. The cyclic voltammograms were recorded using a potentiostat/galvanostat (PGSTAT 30, Autolab, Eco-Chemie, the Netherlands) and the ferrocene was used as a calibration internal standard. The HOMO and LUMO energy levels of the sensitizers were constructed from the oxidation potential and the absorption edge obtained from the UV/Vis absorption spectra.

2.4. Semiempirical computation

Molecular frontier orbitals and geometry optimizations for free sensitizers were computed using Hyperchem7 program. Geometry optimizations were calculated with ZINDO/1 parameter set [27]. The overlap weighting factors were set as a default [21].

2.5. General procedures for preparation of TiO_2 electrodes and fabrication of the DSC devices

TiO_2 were prepared by sol-gel process in an acidic medium according to the literatures [28,29]. Titanium (IV) isopropoxide (TTIP, 98% (72 ml)) was added to 0.1 M HNO_3(aq) (430 ml) with constant stirring at 85 °C for 8 h. When the mixture was cooled down to room temperature, the resultant colloid was isolated by filtration. The filtered colloid was then heated in an autoclave at 240 °C for 12 h to crystallize the TiO_2 colloid. The TiO_2 colloid (with the particle size of *ca.* 20 nm) solution was concentrated to 13 wt% and then 30 wt% (with respect to TiO_2) of PEG (MW = 200,000 or 20,000) was added to form TiO_2 paste. The detailed preparation steps of TiO_2 electrodes using these TiO_2 pastes, the electrolyte composition, the DSSC fabrication procedures as well as the cell performance and properties test are the same as reported previously [25,26]. The sintered TiO_2 electrodes with the active area of 0.16 cm^2 and 20 μm in thickness were selected and immersed respectively in solution of **CYC-B5** (2×10^{-4} M), **CYC-B1** (2×10^{-4} M) and **N3** (2×10^{-4} M) in acetonitrile and *tert*-butylpyridine (the volume ratio is 1:1) for overnight. A Pt-coated (thickness of 100 nm) indium tin oxide glass (ITO, sheet resistivity of 8–10 Ω/square) plate was used as the counter electrode and the electrolyte was composed of 0.5 M lithium iodide, 0.05 M iodine, 0.5 M *tert*-butylpyridine in acetonitrile. In order to avoid the electrolyte leakage, the DSSC cell was fabricated by keeping an ionomer resin (Surlyn 1702, Dupont, thickness of 80 μm) between the two electrodes and two holes were made on the resin. The whole cell was heated at 80 °C on a hot plate until the resin had melted. After the cell was cooled to room temperature, the electrolyte was injected into the space between the two electrodes through two holes. These two holes were later sealed completely with the Torr Seal® cement (Varian, MA, USA).

2.6. The modification of TiO_2 electrode to increase the efficiency of the CYC-B5 sensitized cell

To fabricate the modified TiO_2 electrode, TTIP was first well-mixed with ME (methoxylethanol) (in the weight ratio of 1:3) to make the metallorganic solution. The metallorganic solution was then spin-coated onto the clean conducting FTO (fluorine-doped tin oxide) glasses, followed by annealing at 500 °C for 30 min to form a thin TiO_2 compact layer. On top of this compact film, three layers of TiO_2 paste were coated. TiO_2 paste (Paste1) for the first layer is 20 nm TiO_2 particles mix with PEG (MW of 200,000); second layer paste (Paste2) contains 20 nm TiO_2 particles and PEG with MW of 20,000. Paste2 mixed with 300 nm TiO_2 particles

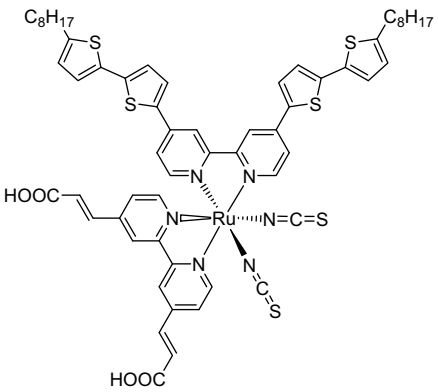

Fig. 1. Molecular structure of **CYC-B5**.

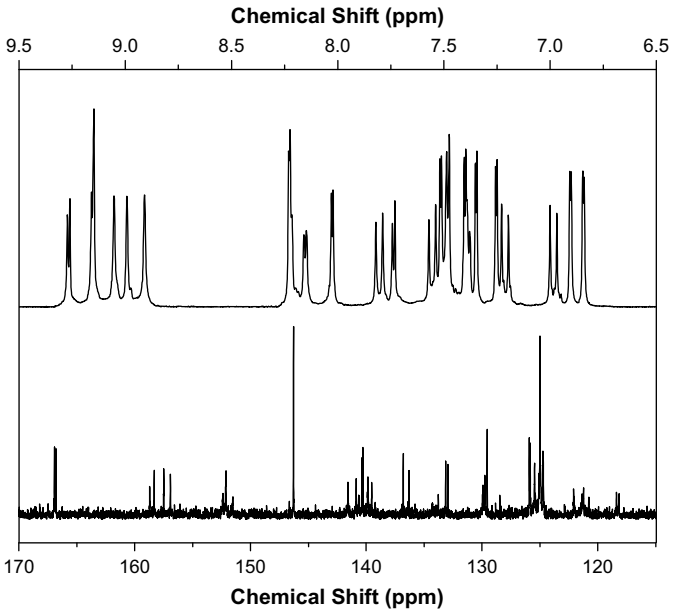

Fig. 2. ^{1}H NMR (aromatic region, top trace) and ^{13}C NMR (at 115–170 ppm region, bottom trace) spectra of **CYC-B5** in d_6-DMSO.

(30 wt% in total TiO_2) was used to coat the third (finial) layer. After sintering at each coating step, TiO_2 electrode with an active surface area of 0.16 cm^2 and thickness of 15 μm was obtained. The TiO_2 electrode was then immersed in the dye solution for overnight. The processes for the device fabrication and photovoltaic performance measurements were carried out using the same procedures as described above.

3. Results and discussion

3.1. Synthesis, characterization and physical properties of *CYC-B5*

CYC-B5 is prepared by a typical one-pot synthetic procedure and its structure is displayed in Fig. 1. The structure of **CYC-B5** can be regarded as an insertion of a vinyl group on the anchoring ligand of **CYC-B1** [25] or as incorporating of vinyl groups on the anchoring ligand and extending the conjugation length of the ancillary ligand with bithiophene units on **N3** dye. The molecular structure of **CYC-B5** was confirmed with ^{1}H- and ^{13}C-NMR spectra (see Fig. 2), Mass and Elemental Analysis. The complicated ^{1}H NMR multi-peaks in the aromatic region revealed that the four pyridyl rings in two different bidendate ligands are magnetically nonequivalent. The peaks at 7.80, 7.55, 7.21 and 6.98 ppm (correspond to the vinyl protons) with the coupling constant of 15.9 ~ 16.0 Hz suggested that the protons in the vinyl groups are in a *trans*-configuration [30]. The ^{13}C NMR spectrum (Fig. 2b) has 44 resonance signals between 110 ~ 170 ppm. These peaks belong to 42 chemically and magnetically nonequivalent carbon atoms in the four pyridyl rings, four thienyl rings, vinyl groups, and carboxylic acids. The other two signals displayed at 133.13 and 132.95 ppm are assigned to the carbons of the two NCS ligands, which proved that the coordination site of NCS ligands is the nitrogen atom.

The geometrical optimization of the calculated frontier orbitals is shown in Fig. 3. The LUMO (lowest unoccupied molecular orbital) is localized on the dcvbpy anchoring ligand, facilitating the electron injection from the photo-excited Ru-complex to the conduction band of TiO_2. The HOMO (highest occupied molecular orbital) and HOMO-1 are contributed primarily from the ruthenium metal center and the NCS ligands, facilitating the MLCT transition. The charge transfer between the metal center (HOMO) and the anchoring ligand (LUMO) has a large effect on the conversion

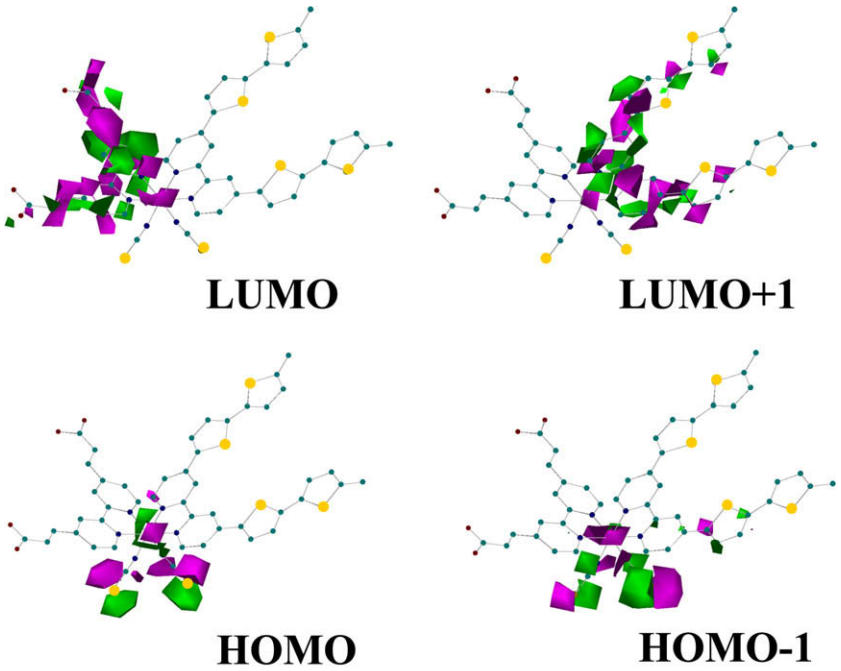

Fig. 3. Graphical representation of the frontier orbitals for **CYC-B5** (O: red, S: yellow, C: green, N: blue, Ru: gray).

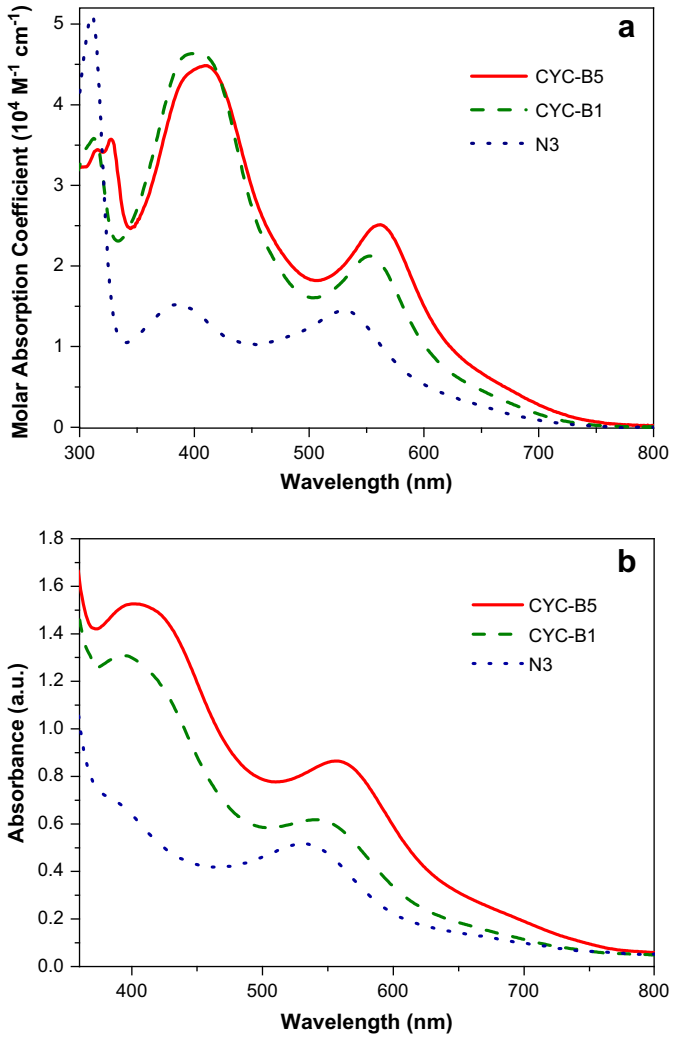

Fig. 4. (a) The electronic spectra of **CYC-B5**, **CYC-B1** and **N3** measured in DMF. (b) The absorption spectra of these three dyes adsorbed,individually on 3.6 μm thick transparent nanocrystalline TiO_2 films.

efficiency of the DSSC device. The proper location of the frontier orbitals also accounts for the high absorption coefficient of the MLCT band for **CYC-B5**. The similar distribution of HOMO and LUMO in **CYC-B5** and **CYC-B1** [25] suggested that by appropriately elongating the conjugation length of the anchoring ligand, the localization of the frontier orbitals for ruthenium complex will not change significantly. **CYC-B5** can be expected to have the similar electron excitation process under the illumination of sunlight and therefore has the light-harvesting ability as good as **CYC-B1**.

The electronic absorption spectra of **CYC-B5** as well as **CYC-B1** and **N3** in DMF are displayed in Fig. 4a and the optical data are summarized in Table 1. The absorption spectrum of **CYC-B5** shows three absorption bands centered at 562 nm (band I), 411 nm (band II) and 327 nm (band III), respectively. The absorption in the UV light region (band III) is assigned to the intra-ligand π–π* transition of dcvbpy anchoring ligand. The band II involves two components: the π–π* transition of ancillary ligand abtpy and one of the MLCT transition bands of the complex. The lowest energy absorption band (band I) is attributed mainly to the metal-to-ligand (anchoring) charge transfer transition of the dye molecule. The λ_{max} of the band I for **CYC-B5** red-shifted 9 nm compared to **CYC-B1**, which is attributed to the extending in the conjugation length on the anchoring ligands. Most importantly, band I has a remarkably high molar absorption coefficient of $2.51 \times 10^4\ M^{-1}\ cm^{-1}$ which is 18% higher than that of **CYC-B1**. These results support that by extending the π-conjugation length of the anchoring ligand, the light-harvesting capacity of the complex could be enhanced and at the same time red-shifted the MLCT band. Furthermore, the electronic absorption spectra (Fig. 4b) of the dyes assembled TiO_2 thin films (4 μm) show that the λ_{max} of MLCT bands for both **CYC-B5** and **CYC-B1** adsorbed on TiO_2 blue-shifted slightly compared to those in DMF, suggesting that there is no multiple layer adsorption of the dye on TiO_2. It is interesting to note here that although the size of **CYC-B5** is larger than **CYC-B1** and **N3**, more **CYC-B5** molecules were adsorbed on TiO_2 electrode (2.24×10^{-8} mol *vs.* 2.02×10^{-8} mol and 2.06×10^{-8} mol for **CYC-B1** and **N3**, respectively, obtained by desorbing the dye molecules from the practical TiO_2 electrodes). Insertion a vinyl group in-between the carbonyl and bipyridine moieties of the anchoring ligand can force the bulky bipyridine moiety to locate far away from TiO_2 surface, results in adsorbing more sensitizers on TiO_2 electrode. If most of the excited electrons on the sensitizers can transfer to TiO_2 efficiently, we can expect **CYC-B5** based cell will have higher current density.

The energy level of the HOMO and LUMO of the dye molecule play an important role in the electron transfer process: the energy level of the LUMO should well match the TiO_2 conduction band edge to assist in electron injection and minimize energetic losses during the electron transfer process [31]; the HOMO should sufficiently positive so that the photo-oxidized dye molecules can be regenerated efficiently *via* electron donation from the electrolyte [32]. To evaluate the energy level of the HOMO and LUMO, the cyclic voltammogram (CV) (shown in Fig. 5) of **CYC-B5** was measured in a DMF solution using $TBABF_4$ as a supporting electrolyte and the resulting data are also summarized in Table 1. **CYC-B5** has two oxidation peaks (at 0.27 V and 0.58 V vs. Fc^+/Fc, as shown by the arrows): The first peak is assigned to the oxidation of the metal center and the second peak comes from the oxidation of the ancillary ligand. The oxidation potential of the metal center in **CYC-B5** shifted only 0.03 V cathodically compared to that of **CYC-B1** since two dyes have the same ancillary ligand. As seen in Fig. 5, the

Table 1
Physical data of the dye molecules and the photovoltaic performance of their corresponding DSSCs.

Sensitizer	ε [*10^4 M^{-1} cm^{-1}] (λ_{max} [nm])			HOMO[a]	LUMO[a]	Cell performance[b]			
	π–π*	π–π* or 4d–π*	4d–π*	(ev)	(ev)	*Jsc* (mA/cm^2)	*Voc* (mV)	*FF*	η (%)
CYC-B5	3.44 (316) 3.57 (327)	4.48 (411)	2.51 (562)	5.07	3.56	20.1	680	0.638	8.71
CYC-B1[c]	3.58 (312)	4.64 (400)	2.12 (553)	5.10	3.52	19.5	669	0.656	8.55
N3[c]	5.11 (311)	1.52 (385)	1.45 (530)	5.20	3.52	18.1	692	0.662	8.29

[a] The electrochemical experiments are carried out in 0.1 M $TBABF_4$/DMF solution to obtain the E_{ox} value. The energy levels of HOMO and LUMO are calculated with the following formula: HOMO (eV) = E_{ox}−$E_{Fc/Fc+}$ + 4.8; LUMO (eV) = HOMO−E_g. E_g is the absorption threshold of the Ru-complexes.

[b] The cell performance of three dyes is measured under the AM 1.5 simulated sunlight illumination (100 mW/cm^2). (Thickness of TiO_2: 20 μm; cell active area tested with mask: 0.16 cm^2).

[c] The physical data of **CYC-B1** and **N3** are collected from our previous report [22].

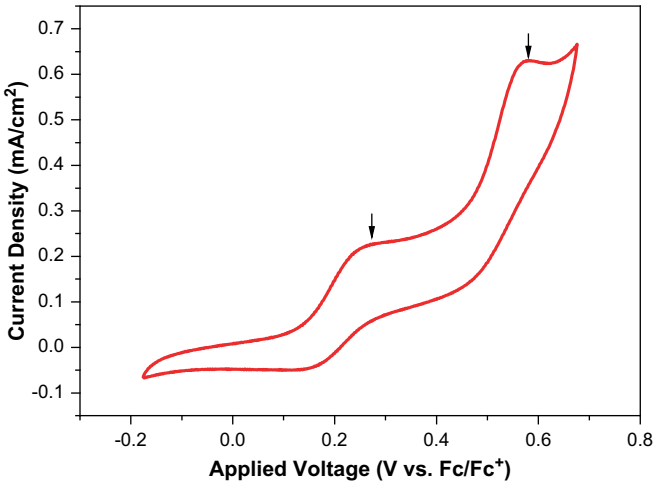

Fig. 5. The cyclic voltammogram (CV) of **CYC-B5** in DMF.

oxidation of **CYC-B5** is not reversible. This is due to that the oxidation potential of thiocyanate ligand is close to that of Ru^{2+} as reported by Grätzel et al. for other ruthenium dyes [33]. Although the energy difference between the LUMO and TiO_2 conduction band edge for **CYC-B5** and **CYC-B1** is similar, **CYC-B5** may still face the dilemma of high absorption but relatively lower electron injection efficiency as proposed by Grätzel et al. [24]. May the gain in the absorption coefficient compensate the loss in the electron injection? The answer may not be trivial.

3.2. The photovoltaic performance of CYC-B5 dye

The *I-V* characteristic curves for **CYC-B5**, **CYC-B1**, and **N3** based DSSCs under AM (air mass) 1.5 sunlight illuminating (100 mW/cm^2) are displayed in Fig. 6. The detailed photovoltaic parameters are also listed in Table 1. **CYC-B5** sensitized solar cell gives a high short-circuit photocurrent density (*Jsc*) of 20.1 mA/cm^2, 680 mV for the open circuit potential (*Voc*) and fill factor (*FF*) of 0.638, yielding the power conversion efficiency (η) of 8.71% which is slightly higher than those of the **CYC-B1** (8.55%) and **N3** (8.29%) sensitized cells under the same device fabrication and efficiency measuring procedures. In addition to the increasing in the photocurrent density, the Voc value of the **CYC-B5** based cell is also slightly

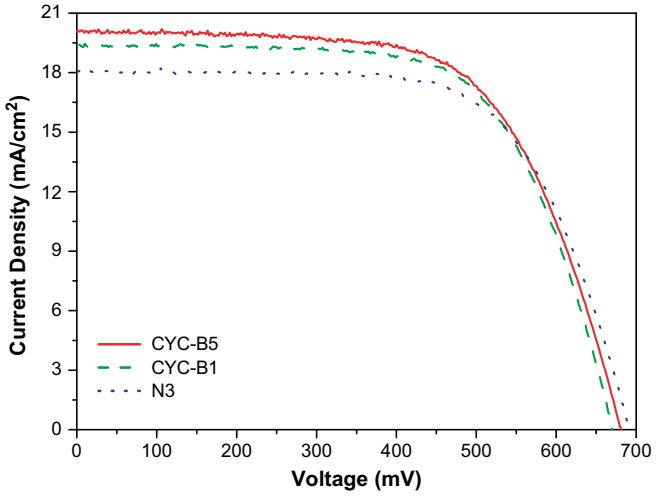

Fig. 6. Characteristic current density–voltage curves of the DSSC devices using **CYC-B5**, **CYC-B1** or N3 as a sensitizer under AM 1.5 simulated sunlight illumination (100 mW/cm^2). (Thickness of TiO_2: 20 μm; cell active area tested with mask: 0.16 cm^2).

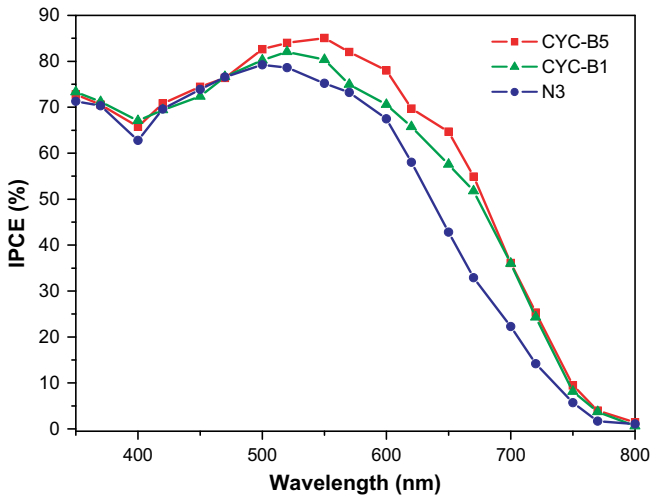

Fig. 7. IPCE spectra of **CYC-B5**, **CYC-B1** or N3 based DSSC devices. (Thickness of TiO_2: 20 μm; cell active area tested with mask: 0.16 cm^2).

higher than that of **CYC-B1** based cell. These photovoltaic data may suggest that the electron recombination of the cell based on **CYC-B5** is less than that of **CYC-B1** based cell. The decreasing in the electron recombination of **CYC-B5** sensitized cell was further supported by the lifetime of the electrons on TiO_2. The lifetime of the electrons on TiO_2 explored with the photoelectrochemical impedance spectroscopy (PEIS) will be discussed further later in the article. The incident photon-to-current conversion efficiency (IPCE) spectra of **CYC-B5**, **CYC-B1**, and **N3** sensitized solar cells are illustrated in Fig. 7. The broad peaks cover nearly the entire visible spectrum from 400 to 700 nm with the maximum of 85.1% at 550 nm, 82.1% at 520 nm, and 79.2% at 500 nm for **CYC-B5**, **CYC-B1**, and **N3** sensitized solar cells, respectively. These data reveal that enriching the MLCT transition of the ruthenium complex (and therefore its performance) can be achieved by properly tuning the structure of the anchoring and ancillary ligands simultaneously.

Photoelectrochemical impedance spectroscopy (PEIS) has been used to study the ion diffusion in the electrolyte, the charge transfer at the counter electrode and the recombination of the electrons on the TiO_2 electrode of a DSSC device [34,35]. We used this technology to investigate the effect of the sensitizer on the lifetime (τ) of the electron on TiO_2 electrode. The τ values for **CYC-B5**, **CYC-B1**

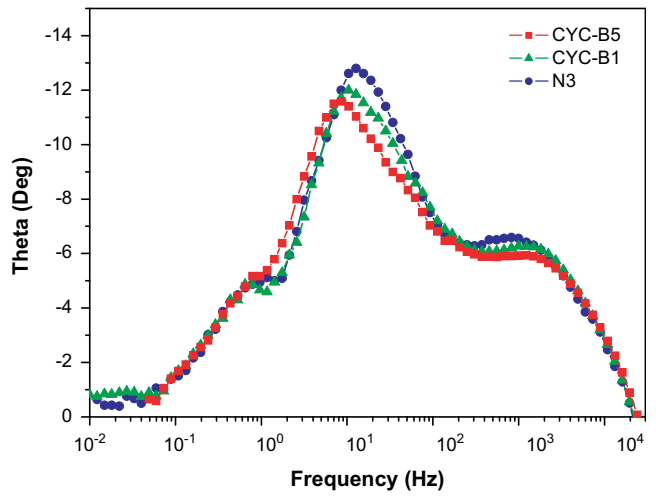

Fig. 8. Photoelectrochemical impedance spectra of **CYC-B5**, **CYC-B1** and N3 sensitized cells in the form of Bode phase plot. (Measured under open-circuit conditions and AM 1.5 simulated sunlight illumination (100 mW/cm^2)).

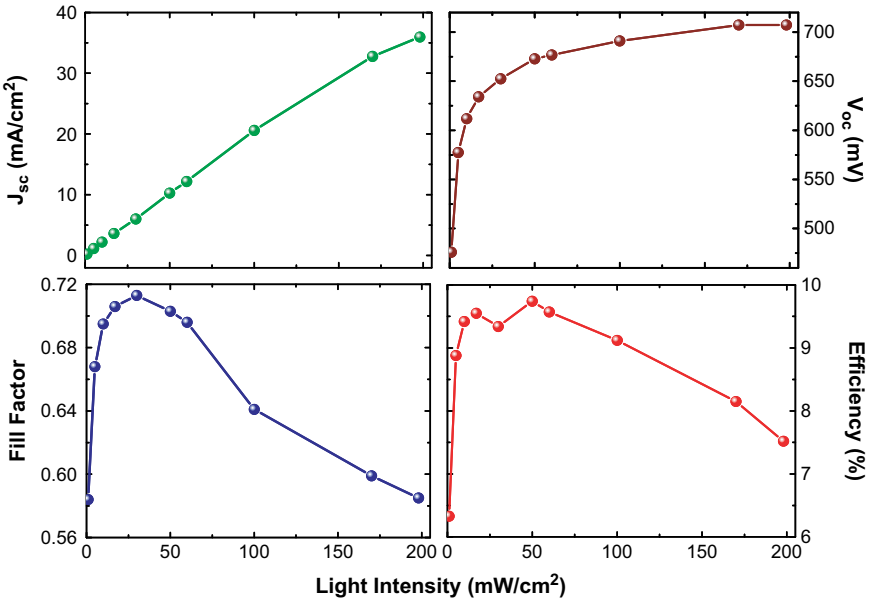

Fig. 9. The effect of the incident light intensities on the J_{sc}, V_{oc}, *FF*, and η of **CYC-B5** sensitized cell. (Thickness of modified TiO_2 film: 15 μm; cell active area tested with mask: 0.16 cm^2).

and **N3** sensitized cells calculated from the intermediate-frequency regime of the Bode phase plot (Fig. 8) are 18.6 ms, 15.3 ms and 14.6 ms, respectively. According to the previous study [24,30], the insertion of the vinyl group in the anchoring ligand does not reduce significantly the electronic coupling between the TiO_2 electrode and the dye cation. Nevertheless, **CYC-B5** sensitized cell still shows a remarkable longer τ value compared to **CYC-B1** sensitized cells. This result suggests that the existence of a vinyl group between the bipyridine and carbonyl group of the anchoring ligand can retard the electron transferring from TiO_2 to the I_3^- ions in the electrolyte.

3.3. The modification of TiO_2 electrode for higher photovoltaic performance

The photovoltaic data showed that the higher absorption coefficient and larger amount of adsorbed **CYC-B5** on TiO_2 were not totally revealed on the current density of the DSSC based on it. The mole ratio of **CYC-B5** and **CYC-B1** absorbed on TiO_2 is 1.11 (**CYC-B5** even has a higher absorption coefficient), but the current density of **CYC-B5** based cell is only 1.03 times of that for **CYC-B1** based cell. This phenomenon may due to the inefficient electron injection of the **CYC-B5** (since a vinyl moiety was inserted in-between the bipyridine and COOH anchoring group) or some electrons are lost before moving to the outer circuit. Therefore facilitating the movement of the electrons on TiO_2 will be the way to increase the conversion efficiency of the device. In order to optimize the TiO_2 electrode, the thickness of TiO_2 electrode was reduced from typical 20 μm to 15 μm and at the same time an additional TiO_2 compact layer (a couple of hundred nm in thickness) was inserted in-between the transparent conducting oxide (FTO) and micro-porous TiO_2 layer. There are various ways to deposit a compact TiO_2 blocking layer on FTO glass, such as spray pyrolysis [36], electro-deposition [37] and so on. In this study, we used a new method named metallorganic deposition method (MOD) in which the titanium isopropoxide was dissolved in 2-methoxylethanol to form a metallorganic solution as a TiO_2 precursor.The detailed studies on how the compact TiO_2 layer affects the properties of TiO_2 electrodes and the resulting performance of DSSC devices will be published elsewhere. The J_{sc}, V_{oc}, *FF*, and overall conversion efficiency (η) of the modified cell based on **CYC-B5** under AM 1.5 simulated sunlight illumination (100 mW/cm^2) are 20.6 mA/cm^2, 691 mV, 0.641, and 9.12%, respectively. The increase in the efficiency may be due to that the TiO_2 compact layer can reduce the dark current of the device as has been observed previously [38] or the electrons can move to the external electrode faster due to the thinner TiO_2 electrode. Furthermore, **CYC-B5** based cell also has good conversion efficiency at high light intensity, due to its notable light-harvesting ability. Fig. 9 shows the photovoltaic performance parameter (J_{sc}, V_{oc}, *FF*, and η) *versus* incident light intensity of **CYC-B5** sensitized cell. The J_{sc} increases almost linearly with the increasing in the incident light intensity up to 198 mW/cm^2, indicating that both the photo-oxidization and regeneration (by the I^-/I_3^- ions) of the adsorbed dye molecules are very efficient. The V_{oc} increases slightly as the light intensity increased, approaching to 710 mV at the light intensity of 198 mW/cm^2 and decreases significantly only when the light intensity is lower than 5 mW/cm^2. Nevertheless, the *FF* at high light intensity decreases substantially, due to the Ohmic losses in the cell. Therefore the overall conversion efficiency reaches its maximum of 9.74% at 50 mW/cm^2 but remains as high as 7.50% at the light intensity up to 198 mW/cm^2.

4. Conclusion

In conclusion, we report the photovoltaic performance of a new heteroleptic ruthenium complex dye, **CYC-B5**, in which the conjugation length of both ancillary and anchoring ligands were extended with a conjugated moiety. **CYC-B5** has the remarkably strong absorption coefficient of 2.51 × 10^4 M^{-1} cm^{-1} for its metal-to-ligand charge transfer band. The conversion efficiency of the DSSC based on **CYC-B5** is better than those based on **CYC-B1** and **N3** under the same cell fabrication and measuring conditions. The photovoltaic data of **CYC-B5** sensitized DSSC have demonstrated that the existence of a vinyl group between the bipyridine and carbonyl segments of the anchoring ligand can not only enhance the light-harvesting ability of the sensitizer but also increase the amount of the sensitizer adsorbed on TiO_2. Furthermore, due to the super-high light-harvesting ability, **CYC-B5** sensitized cell has conversion efficiency higher than 7.50% at the light intensity as high as 198 mW/cm^2 and thin TiO_2 electrode.

Acknowledgments

The financial support from the National Science Council, Taiwan, ROC *via* a grant number of NSC-95-2113-M-008-011-MY3 and from the Photovoltaics Technology Center, Industrial Technology Research Institute (ITRI) were great acknowledged.

References

[1] O'Regan B, Grätzel M. A low-cost, high-efficiency solar cell based on dye-sensitized colloidal TiO_2 films. Nature 1991;353:737–9.
[2] Nazeeruddin MK, Kay A, Rodicio L, Humpbry-Baker R, Miiller E, Liska P, et al. Conversion of light to electricity by cis-X_2bis(2,2′-bipyridyl-4,4′-dicarboxylate)ruthenium(II) charge- transfer sensitizers (X = Cl–, Br–, I–, CN–, and SCN–) on nanocrystalline titanium dioxide electrodes. Journal of the American Chemical Society 1993;115:6382–90.
[3] Horiuchi T, Miura H, Sumioka K, Uchida S. High efficiency of dye-sensitized solar cells based on metal-free indoline dyes. Journal of the American Chemical Society 2004;126:12218–9.
[4] Sreejith S, Carol P, Chithra P, Ajayaghosh A. Squaraine dyes: a mine of molecular materials. Journal of Materials Chemistry 2008;18:264–74.
[5] Nazeeruddin MK, Péchy P, Renouard T, Zakeeruddin SM, Humphry-Baker R, Comte P, et al. Engineering of efficient panchromatic sensitizers for nanocrystalline TiO_2-based solar cells. Journal of the American Chemical Society 2001;123:1613–24.
[6] Islam A, Sugihara H, Yanagida M, Hara K, Fujihashi G, Tachibana Y, et al. Efficient panchromatic sensitization of nanocrystalline TiO2 films by β-diketonato ruthenium polypyridyl complexes. New Journal of Chemistry 2002;26:966–8.
[7] Wang P, Humphry-Baker R, Moser JE, Zakeeruddin SM, Grätzel M. Amphiphilic polypyridyl ruthenium complexes with substituted 2,2′-dipyridylamine ligands for nanocrystalline dye-sensitized solar cells. Chemistry of Materials 2004;16:3246–51.
[8] Chen CY, Chen JG, Wu SJ, Li JY, Wu CG, Ho KC. Multifunctionalized ruthenium-based supersensitizers for highly efficient dye-sensitized solar cells. Angewandte Chemie 2008;120:7452–5. Angewandte Chemie International Edition 2008; 47: 7342-7345.
[9] Hara K, Kurashige M, Dan-oh Y, Kasada C, Shinpo A, Suga S, et al. Design of new coumarin dyes having thiophene moieties for highly efficient organic-dye-sensitized solar cells. New Journal of Chemistry 2003;27:783–5.
[10] Horiuchi T, Miura H, Uchida S. Highly-efficient metal-free organic dyes for dye-sensitized solar cells. Chemical Communications 2003:3036–7.
[11] J. Thomas KR, Lin JT, Hsu YC, Ho KC. Organic dyes containing thienylfluorene conjugation for solar cells. Chemical Communications 2005:4098–100.
[12] Kuang D, Uchida S, Baker RH, Zakeeruddin SM, Grätzel M. Organic dye-sensitized ionic liquid based solar cells: remarkable enhancement in performance through molecular design of indoline sensitizers. Angewandte Chemie 2008;120:1949–53. Angewandte Chemie International Edition 2008; 47: 1923-1927.
[13] Burke A, Mende LS, Ito S, Grätzel M. A novel blue dye for near-IR 'dye-sensitised' solar cell applications. Chemical Communications 2007:234–6.
[14] Wang ZS, Li FY, Huang CH, Wang L, Wei M, Jin L-P, et al. Photoelectric conversion properties of nanocrystalline TiO_2 electrodes sensitized with hemicyanine derivatives. Journal of Physical Chemistry B 2000;104:9676–82.
[15] Wang ZS, Li FY, Huang CH. Highly efficient sensitization of nanocrystalline TiO_2 films with styryl benzothiazolium propylsulfonate. Chemical Communication 2000:2063–4.
[16] Wang ZS, Li FY, Huang CH. Photocurrent enhancement of hemicyanine dyes containing RSO_3^- group through treating TiO_2 films with hydrochloric acid. Journal of Physical Chemistry B 2001;105:9210–7.
[17] Choi H, Baik C, Kang SO, Ko J, Kang MS, Nazeeruddin MK, et al. Highly efficient and thermally stable organic sensitizers for solvent-free dye-sensitized solar cells. Angewandte Chemie 2007;120:333–6. Angewandte Chemie International Edition 2007; 47: 327–330.
[18] Campbell WM, Jolley KW, Wagner P, Wagner K, Walsh PJ, Gordon KC, et al. Highly efficient porphyrin sensitizers for dye-sensitized solar cells. The Journal of Physical Chemistry C 2007;111:11760–2.
[19] Polo AS, Itokazu MK, Iha NYM. Metal complex sensitizers in dye-sensitized solar cells. Coordination Chemistry Reviews 2004;248:1343–61.
[20] Wang P, Zakeeruddin SM, Moser JE, Baker RH, Comte P, Aranyos V, et al. Stable new sensitizer with improved light harvesting for nanocrystalline dye-sensitized solar cells. Advanced Materials 2004;16:1806–11.
[21] Chen CY, Lu HC, Wu CG, Chen JG, Ho KC. New ruthenium complexes containing oligoalkylthiophene-substituted 1,10-phenanthroline for nanocrystalline dye-sensitized solar cells. Advanced Functional Materials 2007;17:29–36.
[22] Jiang KJ, Masaki N, Xia JB, Noda S, Yanagida S. A novel ruthenium sensitizer with a hydrophobic 2-thiophen-2-yl-vinyl-conjugated bipyridyl ligand for effective dye sensitized TiO2 solar cells. Chemical Communications 2006: 2460–2.
[23] Kukrek A, Wang D, Hou Y, Zong R, Thummel R. Photosensitizers containing the 1,8-naphthyridyl moiety and their use in dye-sensitized solar cells. Inorganic Chemistry 2006;45:10131–7.
[24] Klein C, Nazeeruddin MK, Liska P, Censo DD, Hirata N, Palomares E, et al. Engineering of a novel ruthenium sensitizer and its application in dye-sensitized solar cells for conversion of sunlight into electricity. Inorganic Chemistry 2005;44:178–80.
[25] Chen CY, Wu SJ, Wu CG, Chen JG, Ho KC. A ruthenium complex with superhigh light-harvesting capacity for dye-sensitized solar cells. Angewandte Chemie 2006;118:5954–7. Angewandte Chemie International Edition 2006; 45: 5822-5825.
[26] Chen CY, Wu SJ, Li JY, Wu CG, Chen JG, Ho KC. A new route to enhance the light-harvesting capability of ruthenium complexes for dye-sensitized solar cells. Advanced Materials 2007;19:3888–91.
[27] Hirata N, Lagref JJ, Palomares EJ, Durrant JR, Nazeeruddin MK, Grätzel M, et al. Supramolecular control of charge-transfer dynamics on dye-sensitized nanocrystalline TiO_2 films. Chemistry – A European Journal 2004;10:595–602.
[28] Barbé CJ, Árendse F, Comte P, Jirousek M, Lenzmann F, Shklover V, et al. Nanocrystalline titanium oxide electrodes for photovoltaic application. Journal of the American Ceramic Society 1997;80:3157–71.
[29] Nazeeruddin MK, Humphry-Baker R, Liska P, Grätzel M. Investigation of sensitizer adsorption and the influence of protons on current and voltage of a dye-sensitized nanocrystalline TiO_2 solar cell. The Journal of Physical Chemistry B 2003;107:8981–7.
[30] Nazeeruddin MK, Klein C, Liska P, Grätzel M. Synthesis of novel ruthenium sensitizers and their application in dye-sensitized solar cells. Coordination Chemistry Reviews 2005;249:1460–7.
[31] Grätzel M. Conversion of sunlight to electric power by nanocrystalline dye-sensitized solar cells. Journal of Photochemistry and Photobiology A-Chemistry 2004;164:3–14.
[32] Bach U, Lupo D, Comte P, Moser JE, Weissortel F, Salbeck J, et al. Solid-state dye-sensitized mesoporous TiO_2 solar cells with high photon-to-electron conversion efficiencies. Nature 1998;395:583–5.
[33] Yanagida M, Singh LP, Sayama K, Katoh KR, Islam A, Sugihara H, et al. A new efficient photosensitizer for nanocrystalline solar cells: synthesis and characterization of cis-bis(4,7-dicarboxy-1,10-phenanthroline)dithiocyanato ruthenium(II). Dalton Transactions 2000:2817–22.
[34] Schwarzburg K, Willig F. Diffusion impedance and space charge capacitance in the nanoporous dye-sensitized electrochemical solar cell. The Journal of Physical Chemistry B 2003;107:3552–5.
[35] Wang Q, Moser JE, Grätzel M. Electrochemical impedance spectroscopic analysis of dye-sensitized solar cells. The Journal of Physical Chemistry B 2005;109:14945–53.
[36] Sommeling PM, O'Regan BC, Haswell RR, Smit HJP, Bakker NJ, Smits JJT, et al. Influence of a $TiCl_4$ post-treatment on nanocrystalline TiO_2 films in dye-sensitized solar cells. The Journal of Physical Chemistry B 2006;110:19191–7.
[37] Kavan L, O'Regan B, Kay A, Grätzel M. Preparation of TiO_2 (anatase) films on electrodes by anodic oxidative hydrolysis of $TiCl_3$. Journal of Electroanalytical Chemistry 1993;346:291–307.
[38] Cameron PJ, Peter LM. How important is the back reaction of electrons via the substrate in dye-sensitized nanocrystalline solar cells? The Journal of Physical Chemistry B 2005;109:930–6.